Proceedings of the ASME 2010 International Mechanical Engineering Congress & Exposition
IMECE2010
November 12-18, 2010, Vancouver, British Columbia, Canada

IMECE2010-38799

LARGE-SCALE ELECTROSPRAY IONIZATION METHODS FOR NANOCOATING APPLICATION

Marriner H. Merrill
US Naval Research Laboratory
Washington, DC, USA

ABSTRACT

A scalable nano-coating process is needed that can be applied at atmospheric temperatures and pressures with low waste. This would enable the efficient production of advanced thin-film materials from solar cells to super-hydrophobic surfaces. Unfortunately, current methods for producing nanoparticle or nano-structured macromolecular coatings often require substrate immersion, specific atmospheres, and/or long growth times. One potential technique to overcome these challenges would be to use electrospray ionization (ESI) to first disperse large numbers of nanoparticles or polymers in air at standard conditions, and then deposit these on a substrate. ESI is a relatively mature technology, and although it has been developed largely for processing microliter volumes in mass spectrometry, it is believed that the fundamental science can be scaled up. This work presents a model for an ESI deposition method. It combines scaling laws for charged jets with spray and fission models to capture relevant charge, spray, fission, and evaporation phenomena. The developed model is shown to be very simple and efficient while still matching published experimental results. Using the model, current ESI techniques are compared such as NanoESI and Flow-Focusing ESI. A significant technological challenge to ESI deposition is discovered to be the trapping of the majority of the solute in a few primary droplets. Different solutions to this challenge are examined and used to define the direction for future work.

INTRODUCTION

Nanotechnology developments of the last decade have resulted in important potential applications based on thin films or coatings containing nanoparticles and polymers. These new coatings have significant potential effects in both civilian and defense applications. For example, active corrosion protection has been shown using coatings of 'nanocontainers' which release corrosion inhibitors in response to specific external stimuli [1]. Another example is electrochromic films, which change color in response to an applied voltage with very low power consumption [2-3].

While such products have been demonstrated in laboratory settings, real-world products require scalable manufacturing methods capable of applying uniform coatings of nanoparticles, polymers, or other macromolecules over large areas and in roll-to-roll processes. Unfortunately, current technology for processing such films in large quantities or on large substrates is limited. Solution-based methods such as Layer by Layer Self Assembly often require smaller substrate sizes and are limited by diffusion speed [4-7]. Other processing methods, such as sputtering and physical or chemical vapor deposition produce very high-quality films and even achieve fast growth rates under certain limiting conditions (e.g. metallic coatings on the inside of snack-food bags), but are limited to small molecules that can be vaporized [8]. On the other hand, traditional coating methods such as spraying and powder coating have not been able to adequately disperse nanoparticles in air due to clumping [9]. In order to duplicate the simplicity of current spraying methods but with nano-scaled materials, the nanoparticles or polymers have to first be dispersed in a gas, preferably in air at standard temperature and pressure. It is proposed to accomplish this by using a modified form of electrospray ionization (ESI).

A schematic of an ESI deposition system is shown in Figure 1. In all ESI systems droplets with a net charge are produced through some method. The excess charge on the droplets tends to counteract the droplet surface tension, so as the charged droplets evaporate, a critical limit is reached, where the excess charge 'overcomes' the droplet surface tension. This point, known as the 'Rayleigh limit' is then followed by 'Rayleigh fission' of the droplet. During Rayleigh fission, a

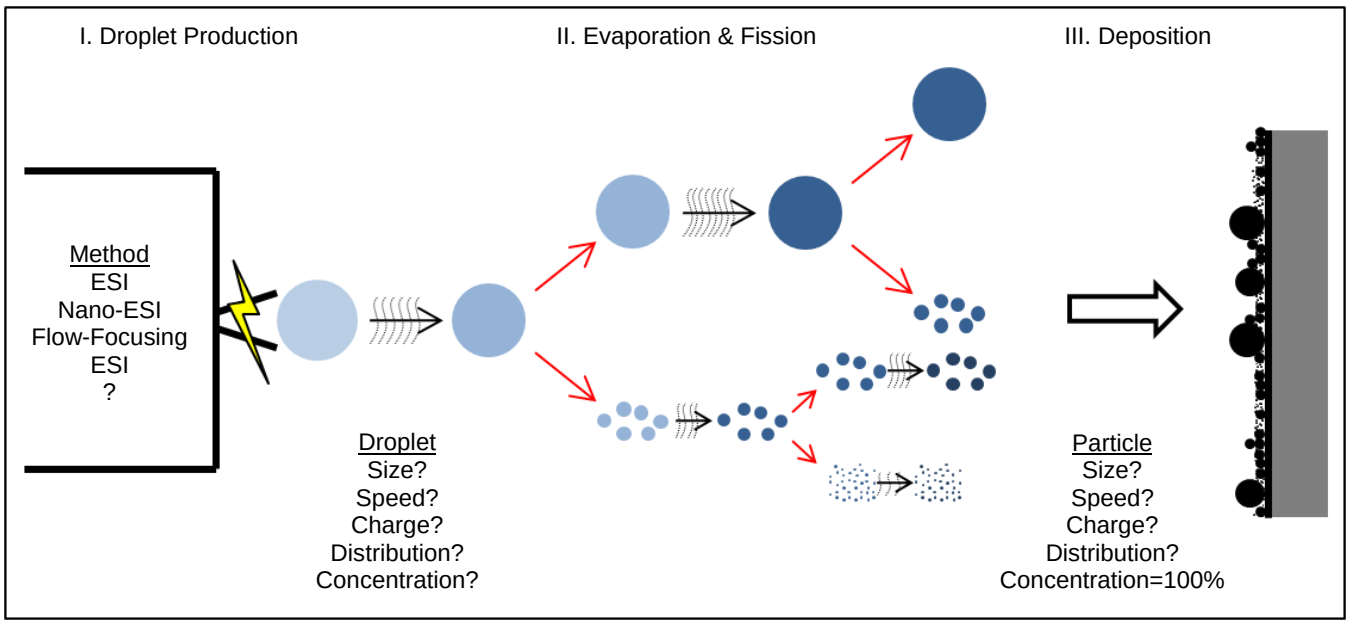

Figure 1. Schematic of a general ESI deposition method showing evaporation and droplet fission.

droplet loses a significant amount of the excess charge with a small amount of mass to several newly created droplets. As evaporation continues both for the original and new droplets, the process is repeated, with the produced droplets eventually reaching the nanometer range. Further droplet fission or direct ion evaporation can result in intact, charged nanoparticles or polymers isolated in the gas, which would finally be deposited. ESI development has been enormously significant in the field of mass spectrometry by enabling the isolation of large molecules such as proteins for analysis [10] and is a standard part of commercial mass spectrometry systems.

While ESI has been demonstrated to coat substrates with polymers [11] or nanoparticles [8,12-13], and even demonstrate patterning [14-15], it has not yet been developed for large-volume applications. Current ESI work often has flow rates on the order of hundreds of nL/min with 0.01% solute concentration [12,16]. In order for a 100 cm^2 surface to be coated with a 1 nm layer in one second, the flow rate and concentration must be increased by a combined 5 orders of magnitude. Some efforts to address this and other shortcomings in ESI have resulted in the development of ESI modifications, including multi-plexing nozzles [17], Nano-ESI [18-19], and Flow-Focusing ESI [20-21].

The objective of this work is to develop a simple model of the ESI deposition process to provide the necessary background for development of a large-scale ESI deposition method. The purposes of such a model are to 1) compare known ESI methods for applicability in deposition, 2) discover potential barriers to large-scale implementation, 3) define the technical challenges, and 4) explore their solution space.

NOMENCLATURE

a	# of primary fission
b	# of secondary fission
B_M	Spalding Mass Number
C_c	Cunningham Correction
d	Jet diameter
$\vec{E}$	Electric Field
I	Current
K	Solution Conductivity
l_m	Mass lost
l_q	Charge lost
n_d	# of child droplets
Nu	Nusselt Number
Pr	Prandtl Number
Q	Volume flow rate
q	Electrical Charge
r	Radius
Re	Reynolds Number
Sc	Schmidt Number
Sh	Sherwood Number
v	Velocity

Greek:

γ	Surface Tension
ε	Permittivity
η	Concentration
λ	Mean Free Path
μ	Viscosity
ρ	Density

Subscripts/Superscripts:

0	State at first fission event
d	droplet
f	Fluid
g	Gas
R	Rayleigh limit
v	vapor
s	surface
∞	far-field

ESI-DEPOSITION MODEL

The Model

Due to the relative maturity of both ESI and traditional spray, there is a significant body of experimental, numerical, and theoretical work to draw from in the creation of a simple model. Good reviews of sprays can be found by Lasheras and Hopfinger [22] and Sazhin [23]. These cover topics ranging from the evaporation of individual droplets to the ensemble spray behavior. For ESI, theoretical works by Ganan-Calvo [24], Fernandez de la Mora [25], and by Collins, Jones, et al. [26] provide excellent 'scaling laws' that describe the production of charged droplets from a jet. Somewhat similar work examining the Rayleigh fission of individual drops has

also been researched with a variety of different experimental or theoretical techniques [27- 31].

Other researchers have focused on the behavior of the cloud of produced droplets, using both Lagrangian and Eulerian frames of reference [32-34]. Published results range from numerical codes that explicitly track each droplet to line-of-charge approximations that allow for numerical solutions of the effect that one spray plume would have on a neighboring spray plume in a multiplexed nozzle system. Finally, a few researchers have focused on the deposition of the droplets [34-36] using similar numerical techniques.

Despite this body of work, there is not yet a simple model that could be used to predict the bulk characteristics of a deposited film. Most of the droplet-tracking or other codes focus on the transport of droplets, neglecting the evaporation or the actual Rayleigh fission process and their effect on the solute concentration [32-33,36-37]. This is quite limiting, since a single micrometer-sized droplet can fission eventually into thousands of deposited particles! At the other extreme, detailed studies of Rayleigh fission are often limited to a single droplet, without developing a model to assess the overall effect

The goal of this work is to bridge the gap, creating a model that includes all vital processes, while still being computationally simple. Through a judicious combination of prior work along with standard spray assumptions and an understanding of the physical processes, the developed model is simple but appears to very effectively capture the spray behavior.

Simply, a droplet is created with an initial size, concentration, velocity, and charge. It then translates in the axial direction evaporating and fissioning to create children droplets until it is deposited on the substrate. In this process, the principal assumptions are:

- Steady-state spray. It is assumed that the spray process, evaporation, etc, do not change over time.
- Uniform electric field. The electric field inside the spray cloud is a combination of the external field and the field created by all of the surrounding droplets. However, it is common to replace this with a line-of-charge model that essentially collapses all of the charges into a single line of charge extending from the nozzle tip to the substrate [32]. Additionally, assuming that the charge density of the cloud does not vary significantly as droplets evolve and translate toward the substrate (i.e. charge is preserved, even if mass and number of droplets change), it is possible to neglect the axial charge variation. Such an assumption is incorrect near the substrate or the nozzle [34], but is good to the first-order.
- Non-interacting droplets. It is assumed that a droplet does not affect other droplets or the surrounding gas. So the evaporation and fission of each droplet occurs as though it were in an infinite media. This is a common assumption for dilute sprays [22].
- The radial location of the droplets is unimportant and droplets are deposited randomly over the substrate. This is not true, as it is well known that ESI sprays have a core of larger droplets surrounded by smaller droplets on the perimeter [34]. However, much of this could be controlled by modifying the local electric field. By neglecting this radial information, the model is significantly simplified into a single dimension without losing any information about the droplet characteristics and evolution.
- There is sufficient distance for all droplets to completely evaporate before arriving at the substrate, with no droplet resolvation [10]. As will be shown, this assumption is very powerful, since it decouples the problem from the evaporation rate.

Using these assumptions, a numerical code was written that tracked each droplet from its source either at the nozzle or as the offspring of a fission event to final deposition on the substrate. Each droplet was allowed to evaporate and fission, while the total droplet mass, solute mass, droplet temperature, and velocity evolved.

Some specific details about the model follow. Except where noted, the assumptions and models used were the simplest widely-accepted options.

Initial Conditions. For ESI-produced droplets, the initial conditions were found using the scaling laws defined by Ganan-Calvo [24] for the most common electrospray regime:

$$I = \sqrt{\gamma K Q}, \qquad d = \left(\frac{\rho \epsilon_g Q^3}{\gamma K}\right)^{1/6} \tag{1}$$

where d is the radius of the jet, and the droplet radius is assumed to be four times the jet diameter. Droplet temperature was assumed to be room temperature, and initial droplet velocity was assumed to be 10 m/s [38], though this was seen to have very little effect on the droplet.

Evaporation. The governing equations for the evaporation of the solute and convection from the droplet were standard evaporation and diffusion models from a spherical drop using the lumped-mass approximation. The Nusselt and Sherwood numbers used were from Sazhin's review [23]:

$$Nu = \begin{cases} Re \le 1 & 1 + (1 + RePr)^{1/3} \\ Re > 1 & 1 + ((1 + RePr)^{1/3}) Re^{0.077} \end{cases} \tag{2}$$

$$Sh = \left(2 + 0.87 Re^{1/2} Sc^{1/3}\right)(1 + B_M)^{-0.7} \tag{3}$$

All dimensionless groups were defined as usual. For clarity, note that the Reynolds and Spalding mass number are

$$Re = \frac{2 v_d r_d \rho_g}{\mu_g}, \qquad B_M = \frac{\rho_{vs} - \rho_{v\infty}}{\rho_{gs}} \tag{4}$$

External Forces. It was assumed that only drag and electrostatic forces acted on the droplet. Stokes drag was used, and subsequent checks on velocity and the Reynolds number showed that this assumption was good. Following Greendyke and Kaplan [33]:

$$F = q_d \vec{E} + \frac{6\pi\mu v r_d}{C_c}\left(1 + \frac{3}{16} Re\right) \tag{5}$$

$$C_c = 1 + \frac{2.52\lambda}{2 r_d} \tag{6}$$

For the simple geometry and atmospheric assumptions, the Cunningham correction (C_c) used 100 nm as the mean free path of the gas. The uniform electric field meant that $\vec{E}$ is a one-dimensional scalar, which was assumed to be $1X10^5$ V/m. This corresponds to kilovolt charge with centimeter axial spacing.

Rayleigh Fission. One of the most important contributions of this model is the inclusion of a simple method for modeling the Rayleigh fission and demonstration of its success. Physically, the electrostatic charge in a droplet works to counteract the surface tension. As evaporation occurs and the droplet shrinks, eventually a point is reached where the surface charge overcomes the surface tension and the droplet breaks apart. This point, known as the 'Rayleigh limit' after Lord Rayleigh is defined as:

$$q_R = 8\pi\sqrt{\epsilon_g \gamma r_d^3} \qquad (7)$$

There is some disagreement about whether the droplet actually fissions at q_R or prior to it, say at 80% of q_R [39]. Also, while it is known that the parent droplet retains the bulk of the mass and the charge during fission, it isn't known exactly how many droplets are created or their charge and size distribution. For this model, the assumptions used appeared to be representative from more detailed models of the fission process [29-31,39] and the results validate them.

Briefly, fission is assumed to happen when q_d reaches q_R, and at that point a fixed number of equally charged child droplets are formed from a fixed percentage of the parent droplet's mass and charge. For the studies presented here, it was assumed that the number of child droplets (n_d) was 6, mass lost from the parent droplet (l_m) was 2%, and charge lost (l_q) was 15%. This gives child droplets with a radius of approximately 15% that of the parent droplet. It was assumed that the temperature and concentration of the parent droplet are unchanged during fission and that each child droplet has the same concentration and temperature as the parent droplet. As mentioned, these assumptions worked very well. Additional information about the theoretical effects of varying these parameters is reported by Tang and Smith [29].

Deposition. This is another key contribution of ESI models. Of greatest interest for future ESI deposition methods is the state of the droplet immediately prior to landing on the substrate. At that point, is all of the solvent evaporated? If so, what is the size of the remaining particle? Is it a single particle, or a clump that has precipitated together? Did evaporation cause the solvent to freeze into a tiny lump of ice [37]? The answers to these questions are based on the solute and solvent, the size and morphology of the solute, and the precise method of ion formation, which is still a matter of debate [10,40].

Numerically, droplets are deposited simply by removing them from the evaporation-fission routine and recording the final information. By multiplying the final mass and concentration and assuming a particle density, the deposited particle size is calculated.

For this model, deposition was based on a critical concentration, not size or location. Essentially, this assumes that at a certain concentration, the solute will precipitate within the droplet into an indivisible aggregate. Such an assumption is physically realistic. The maximum concentration was chosen somewhat arbitrarily as 62%, which corresponds to slightly less than the concentration of randomly packed spheres. This is naturally very system dependant, but by keeping this constant for all cases, comparisons between spray methods can be made.

In addition to the critical concentration, a size criterion was also implemented. This is necessary because the continuum nature of the model would otherwise allow for the non-physical infinite divisibility of solute particles or polymers. Fortunately, to attain the goals of this work, a very simple solution captures the physics. What is most important is to know whether the droplet reached a small enough size with a low enough concentration to form individual, charged nanoparticles. Any particle predicted by the model to be below that size obviously achieved that purpose. To avoid tracking thousands of these unrealistic drops, once a droplet reached a certain minimum size, it was assumed to have deposited. Unless noted otherwise, the cutoff radius used was 3 nm. Varying the cutoff radius to 6 nm was found to have insignificant effects on the results.

Physically, the nanoparticles or macromolecules would have been issued discretely through one of a few different ion formation mechanisms [28], instead of being allowed to subdivide uniformly. To represent this, deposited particles are post-processed by taking all the solute mass deposited in particles of less than a certain radius, and creating a smaller number of larger particles of some logical size, such as the known nanoparticle diameter. This obviously does not change the cumulative mass distribution, since mass is conserved.

Numerical Implementation. Implementation into a numerical code was fairly straightforward, but a couple of points can be made. First, the wide range of droplet sizes means that the time step should also range orders of magnitude. Fortunately, because droplets do not interact, it is possible to set a 'big' time step (on the order of 1/1000 of the expected evaporation time of a droplet) and then allow each droplet to take the necessary number of internal iterations to reach that time, with internal time steps scaled such that less than 1% of a given droplet's mass was lost at each step. Second, because of the steady state and non-interacting assumptions, the flow rate is unimportant. Somewhat arbitrarily, one new primary droplet was released every set time increment. Usually, this was scaled to have approximately 100-1000 primary droplets in the code at any one time, to allow for future flexibility.

Using this scheme, hundreds to tens of thousands of droplets of all sizes and concentration were propagated through repeated evaporation and fission in reasonable time on a desktop computer. The standard procedure was to run the code for long enough that the first droplet produced would have completely deposited. By this point, a steady state in the spray cloud would have been reached. This state would then be used as an initial condition to re-run the process for a short time (usually the time to release two new droplets) and collect deposition information. Depending on the initial droplet size and

A.

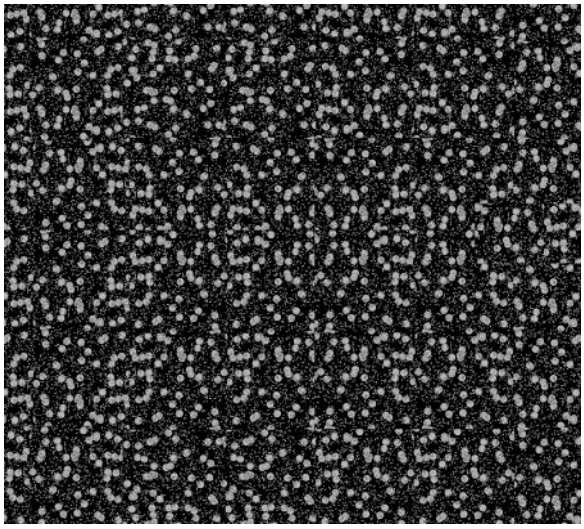

B.

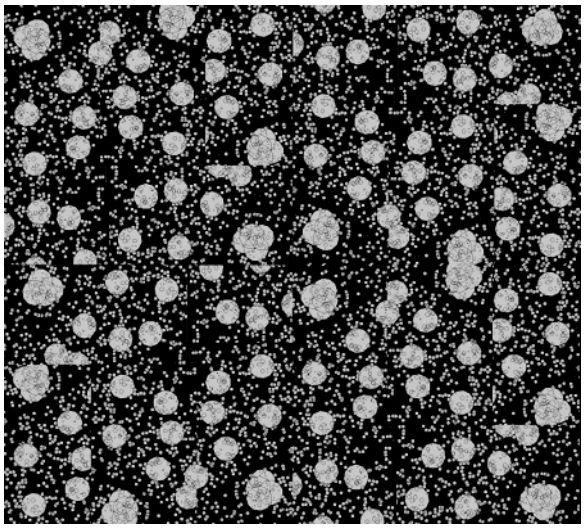

Figure 2. Particle distributions generated by the numerical model imitating the experiments of Lee, Kim, et al. [12]. A) relates to the low concentration case, and B) to the high.

concentration, each droplet resulted in the deposition of thousands to tens (and even hundreds) of thousands of particles. This deposited droplet information was post-processed to create mass and number statistical distributions for the variables of interest (temperature, concentration, charge, etc.).

Validation

The model was validated with a test case using the inputs and results from experimental work published by Lee, Kim, et al. in 2007 [12]. In their experiment, a solution of FePt nanoparticles with an initial diameter of 2.5 nm was electrosprayed onto a substrate under two different conditions. In the first case, 0.01% FePt in a hexane-solution was mixed with ethanol (50/50, v/v) and sprayed at a rate of 200 nL/min with a positive voltage of about 5 kV and a distance to the counter electrode of about 2 cm. In the second case, 0.1% FePt in a hexane solution was mixed with ethanol (20/80, v/v) and sprayed at 800 nL/min.

The inputs for the model developed here were found by first using the scaling given in Equation 1 to find the initial droplet diameter and the charge carried by each droplet. Fluid properties were assumed to be those of pure ethanol (conductivity of 1.1X10-4 S/m). The result was drops with a diameter of 2.8 μm charged to $9.4X10^{-15}$ C (51% of q_R) and 5.2 μm charged to $3.76X10^{-14}$ C (80% of q_R) for cases one and two, respectively. Other experimental inputs included initial concentration of 0.1% and 0.01% and an external temperature of 375 K.

The deposition results showed excellent agreement with experiment without any 'massaging' of the model or the inputs. For the first case, Lee, Kim, et al. reported achieving a fairly monodisperse set of particles with a mean diameter of 5 nm as measured by FE-SEM. For the second, they reported larger particles appeared with a diameter of about 35 nm. This behavior was repeated by the model as can best be seen in Figure 2 showing the two model-generated particle distributions. These are scaled to be directly compared with Figures 4a and 6c in the original paper. Other than slightly higher particle density in the images in this paper, the match between the model and the experimental figures is excellent. In absolute values, the match is also quite good. Compared with the 5 nm and 35 nm particles shown experimentally, the model predicted 10 nm and 67 nm. The 7X increase in size between cases one and two matches well and the 2X discrepancy in absolute values is to be expected due to the assumptions made using the scaling laws and the fact that particle density in the model was assumed to be the same as that of the solvent.

Another very important similarity between the model and experimental results is the existence of at least two very different sizes of particles in a given deposition. Examining Figure 2B in this work and Figure 6C in Lee's paper, both large and small particles are seen together, with no 'medium' sized particles. As will be explained below, the steps in particle sizing are a direct result of Rayleigh fission.

Along with providing excellent validation, the model also gives additional information about the results which are difficult to observe experimentally, particularly at the smaller size. For example, the model predicts a significant number of particles with diameters closer to the original 2.5 nm – 96% of the particles in the first case and 8% of the particles in the second. These were not explicitly reported by Lee, Kim, et al. Experimentally, these must have either absorbed into the larger particles during heating or were not visible in the SEM images. Either way, knowing of their potential existence would be an important key for during experimentation. Note that all of these smaller particles are included in Figure 2. They are difficult to see, particularly in Figure 2B (where the more visible specks are in the 10 nm range), just as would be the case for the real images.

Simplifications

One of the most important outcomes of the above validation is the remarkable conformity with experimental results, even though the solution properties were essentially incorrect, using ethanol alone instead of a 50/50 or even 20/80 ethanol/hexane mix. In fact, switching all material properties to that of water, but leaving the same initial droplet size, charge, and $\%q_R$, gave results that differed by only about 8% - most of that expected to be due to the assumption of particle density being the same as solvent density. In other words, the process of going from charged droplets to final deposition properties does not appear to depend directly on the solvent used.

This observation leads to an important simplification of any process in which evaporation and fission are occurring: *assuming sufficient time for complete evaporation and conservation of charge, the droplet evolution is governed entirely by the fission parameters.* Consider a droplet of volume V_1 charged to the Rayleigh limit. It undergoes fission and loses 2% of the mass and 15% of the charge. Regardless of the solvent, given enough time, the solvent will evaporate down to the point that the droplet is again critically charged. Using Equation 7 the volume right before the next fission event, V_2, can be shown to be a straightforward function of only V_1 and 15% (l_q)! This process can be repeated for any number of fission events. As an equation, it can be shown that the volume of the critically charged droplet after $i=a$ fission events is

$$V_{i=a} = (1 - l_q)^{2a} V_0 \tag{8}$$

With similar manipulations, the critical volume of the child droplets can also be found. As with the parent droplet, it is assumed that the child droplet is formed and then evaporates to the next critical point, where it will have a volume of

$$V^{j=b} = \left(\frac{l_q}{n_d}\right)^{2b} V_0 \tag{9}$$

The superscript on V indicates the number of secondary fission events. So, b=1 means that the droplet is the child of V_0, b=2, means that the droplet under consideration is the grandchild. Continuing the family analogy, a droplet which was a child of the main droplet, and then underwent two parent fission events (i.e. lost mass to children of its own) would have a=2, b=1. Importantly, the order of the 'pedigree' is unimportant in defining droplet size. Re-writing, and repeating the entire process for concentration, it is shown that the droplet size and concentration at the critical limit are very simply and directly related to the number and type of fission events, the fission assumptions (mass lost, charge lost, and number of child droplets formed), and the properties at the first critical drop size. This is shown in Equations 10-11.

This is not to say that solvent properties have no effect. They still do, in three important ways. First, the solvent is vital to whether or not ESI can occur at all. The process of Taylor cone formation and jet ejection are strongly dependent on solvent properties. Second, the solvent properties impact the initial jet size and current flow, seen in the scaling laws in Equation 1. This affects the charge on a droplet, q_d, and that combines with the droplet interfacial tension to define the volume and concentration of the droplet at its first critical size (V_0 and η_0) through Equation 7. Finally, solvent evaporation controls the temperature of the droplet. This is primarily important if the temperature significantly impacts the solubility for the solute or if the solvent freezes. Fortunately, the droplet momentum to drag ratio is such that the droplet relative velocity is quite low and the Nusselt and Sherwood numbers can be approximated to be constant with a magnitude of 2.0. This simplification allows for a closed form solution of the droplet steady state temperature in Equation 12.

To summarize, the following equations represent the much-simplified model of the droplet volume, concentration, and steady-state temperature.

$$V_a^b = (1 - l_q)^{2a} \left(\frac{l_q}{n_d}\right)^{2b} V_0 \tag{10}$$

$$\eta_a^b = \left\{\frac{1 - l_m}{(1 - l_q)^2}\right\}^a \left\{\frac{n_d l_m}{(l_q)^2}\right\}^b \eta_0 \tag{11}$$

$$T_d = T_\infty - \frac{h_{fg} D}{K_g} (\rho_{vs} - \rho_{v\infty}) \tag{12}$$

These three equations are valid for any process in which charged droplets are evaporating and fissioning with conservation of charge. Equations 10 and 11 give the exact same results as the full numerical model, while Equation 12 is an approximation that is generally accurate to within a few degrees.

RESULTS AND DISCUSSION

The first important result from the model is that three parameters and three initial conditions completely describe droplet evolution. These are the Rayleigh fission process parameters (3 independent parameters) and the initial size, concentration, and charge of the droplet. These six parameters are themselves affected by the solvent properties, method of spray, etc., but they are the physical core of the ESI process.

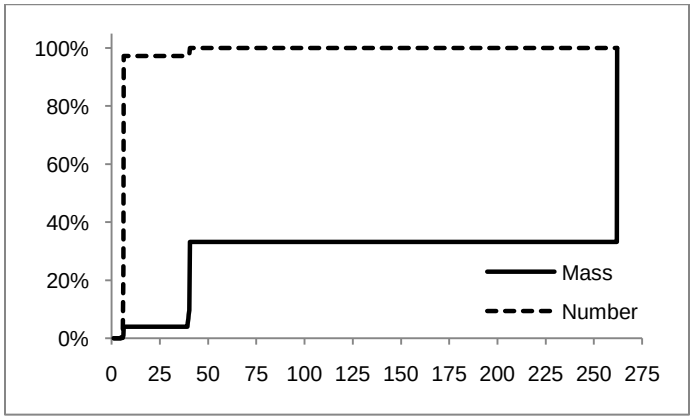

Figure 3. The cumulative number and mass distributions vs. deposited particle diameter (nm) for a typical ESI case.

Table 1. Comparison of Common ESI Methods

Name	*Initial drop diameter (nm)*	*Initial Charge (%q_R)*	*Mass% in particles < 12 nm diameter*	*Diameter of b=0 particle (nm)*	Mass% of *b=0* particle
ES-50	3000	50%	2.3%	267	70%
ES-80	3000	80%	4.0%	262	67%
ES-95	3000	95%	4.5%	260	65%
ES-80b	6000	80%	0.1%	524	67%
EFF	800	31%	25%	72.8	75%
Ag	35000	23%	0.0%	3227	79%
NanoES	300	70%	35%	26.0	65%

The second important result of the model is that it can be used to compare the different ESI processes. Rayleigh fission occurs the same for any drop regardless of how it was created, and all of the methods examined were capable of spraying solutions with the same solute concentrations. So, of the six independent parameters, only two significantly vary between these different processes: the initial droplet size and charge.

Four different electrospray ionization methods were compared: A typical electrospray (ES), combined electrospray and flow focusing (EFF) [21], Nano-electrospray (Nano-ES) [19], and 'agricultural' ESI (Ag). This last is essentially a standard spray nozzle coupled with induction charging of the droplets and is typical of the large-volume sprays sometimes used to spread pesticides [41]. All model and solution parameters were kept constant, with solution concentration at 0.1%. Instead of using scaling laws to get the initial droplet size and charge, these were taken from the literature referenced above. To demonstrate the effect of initial size and charge, ES cases were run with initial charge at 50%, 80%, and 95% of q_R and two different initial drop diameters. The input parameters and the results are summarized in Table 1.

Figure 3 shows the results from a typical run. This was an ESI process with initial drop diameter of 3 μm charged to 80% of q_R (ES-80). The trend of the results was typical for all the processes examined in this study. Since the primary focus of this work is on the characteristics of coating, the number and mass distributions of the deposited particles are most useful. Note that:

- There is an enormous difference between the mass and number distributions. Generally more than 95% of the particles created had diameters less than 5 nm; however these account for a very small proportion of the mass, often less than 1%. As the particle size increases, the situation is reversed.
- The discrete, 'stair-step' nature of the distributions is due to discrete particle size categories. These are a direct function of the Rayleigh fission process. Because the child droplet is so much smaller than the parent droplet very discrete steps are created. So, the various number or mass 'steps' can be traced back to specific secondary fission events. The largest particles come from droplets which have undergone only primary fissions (*b=0*), seen in Figure 3 at about 265 nm. The next largest come from particles which have undergone exactly one secondary fission (*b=1*). If the resolution of the chart allowed, it could be seen that these steps continue even for the smaller particles. Experimentally, natural variations in initial drop size and charge, as well as variability in individual fission events results in some smearing of these steps, but as previously mentioned, we hypothesize that it is largely retained [29].
- A single particle is responsible for a significant fraction of the total mass deposited from each droplet (i.e. the *b=0* particle). It is easy to show that the final mass increase in Figure 3 is a single particle, the remainder of the original drop once the limiting concentration was reached. Using Equation 11, it can be shown that for this case, there were *a=20* fission events, and a final particle with a diameter of 262 nm holding 66.8% of the initial solute mass. This is in exact agreement with Table 1, where the results are from the full evaporation/fission code. The large mass of this single particle has significant quality and waste implications.

The results in Table 1 also yield some important observations about the current ESI methods. First, the different methods result in widely varying initial conditions, with drop diameters from 300 to 35,000 nm. These differences affect the deposition properties as expected. Smaller initial drops with higher charge lead to smaller particles and more uniform coatings. However, regardless of method, the majority of the solute is locked into the *b*=0 particles. And those particles are large. Only EFF and NanoES gave results that were under 100 nm. And even in those cases, the particle was too large to give uniform coatings of nanoparticles on the order of 10 nm. NanoES would seem to be the most promising, but further reduction in initial drop diameter by 2-3 times would come at the expense of even smaller dispensing tips, with increased low-flow and clogging issues.

EXPLORING SOLUTIONS

There are cases where deposition of particles of discrete and very different sizes can be an advantage. For example, some superhydrophobic surfaces in nature consist of bumps on the scale of 10's of micrometers covered with nanostructures at the scale of 100 nm [42]. However, more often, uniform coatings are desirable.

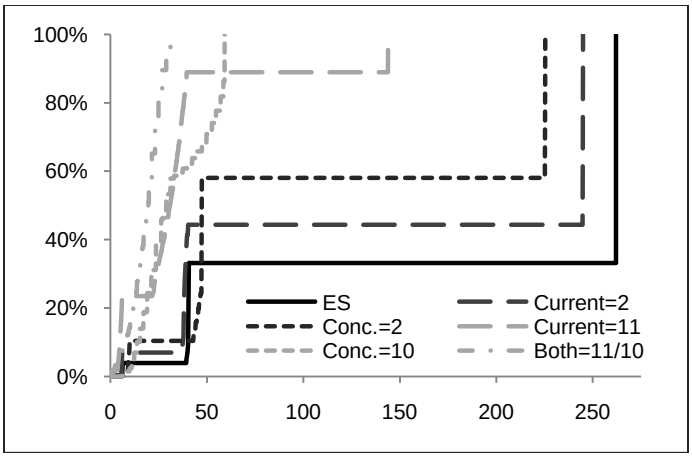

Figure 4. Cumulative mass distributions showing the effect of increased current (from a plasma) and/or increased concentration in children vs. parent droplets.

The simplest solution is to decrease either initial drop size or concentration. Utilizing Equations 10 and 11, it is possible to examine how small of a particle or how low of a concentration would be needed to produce a given maximum allowable particle radius. Given this maximum is 5 nm, consider a low but realistic initial solute concentration of 0.01%. For the droplet to reach the desired end state, the initial droplet radius must be 62 nm, well below current capabilities. Alternately, consider a small but attainable initial droplet radius of 500 nm. The initial concentration would need to be 0.000032%. Neither of these options is viable.

In existing ESI systems for mass spectrometry this large drop issue has primarily been handled using aerodynamic drag or electrostatic forces to control the largest drops. The possible acceleration of a droplet near q_R scales with $\vec{E}/r^{1.5}$ for an applied electric field and v/r^2 with an applied air flow. In each case, the exponent on the radius increases the ability to segregate droplets based on size. Specific challenges to this method include the relatively short time and distance in which to capture and remove the droplets, and the significant complexity of doing this in systems with multiple nozzles or high carrier gas velocity.

Another known solution to this issue is through solvent selection. Physically, most of the material in a child droplet comes from the surface of the parent droplet. In cases where the solute tends to concentrate on the surface of the droplet, child droplets would tend to have higher concentrations of solute than their parent droplet. Two cases were run, one where the solute concentration of the child after fission was 2X that of the parent droplet, and the other where it was 10X. Numerically this was simply done within the fission subroutine, being careful to conserve mass of both solute and solvent. The exact nature of the enriching effect of the surface molecules is much more complex than this [31], but these two cases give an idea of what is possible. And the results in Figure 4 indicate that this is an effective method. As the concentration in the child droplet increased, the diameter of the largest particle reduced from 260 nm to 225 nm to 50 nm.

A new solution to this challenge might be to use a plasma to increase the charge of the droplets during the evaporation/fission stage. Recently, Harper demonstrated that it was possible to use a low-temperature plasma to essentially 'boost' the charge on analyte molecules to aid in transferring them a long distance to a mass-spectrometer unit [43]. Possibly a plasma could be used to increase the charge on the droplets in the spray cloud, encouraging them to reach q_R more quickly and thus undergo more fission events per given evaporation. Computationally, this was modeled by adding charge to each droplet at each time step. Total charge added per time step was set to be equal to a given multiple of the original electrospray current (the initial charge on a droplet multiplied by the droplet flow rate). Also, since plasma-induced charging is a collision process, the charge was apportioned by droplet cross sectional area. The results of using a plasma to increase the total current to 2X or 11X the original current are shown in Figure 4. The plasma did have an effect on the distribution, decreasing the size of the largest particle by a factor of two and the mass locked in that particle from 66% to 12%.

The final curve shown in Figure 1 is from combining the effects of increased current and child solute concentration. This case provided the best scenario, with the largest droplet being only 31 nm and the majority of deposited particles less than 15 nm. While still not a perfect solution, these results indicate that continued research in this and similar areas is warranted. And, the ease of creating and running such tests underscore the usefulness of the developed model.

CONCLUSIONS

An electrospray ionization (ESI) deposition method was proposed as a future, large-scale coating method. To investigate this hypothesis, a model was developed with the goal of 1) comparing known ESI methods for applicability in deposition, 2) discovering potential barriers to large-scale implementation, 3) defining the technical challenges, and 4) exploring their solution space. The developed model is simple and is focused on the parameters most important for future development of a large-scale coating method. It consists of physically based assumptions regarding Rayleigh fission combined with key simplifications and traditional droplet evaporation predictions. Computed results show excellent agreement with published experimental work.

The model results indicate that there are only a few key characteristics of the evaporation-fission process and that they are inherent in any system of charged droplets experiencing evaporation. These characteristics are the Rayleigh fission parameters (here simplified to 3 independent variables) and the droplet initial size, concentration, and charge. Additionally, it was shown that many of the most important characteristics, such as final particle size, can be solved directly by hand.

The model was used to compare four current electrospray methods. In each case, more than 60% of the solute never escaped the original droplet, forming a large particle clump.

This poses problems of waste and surface quality for future coating methods. Solutions to this problem were examined utilizing the model. Both adding charge to the droplets using a plasma and enriching the solute concentration in child droplets during fission were somewhat effective in reducing the size of these large particles. A combination of these two methods performed even better. Future work exploring these and other solutions both experimentally and computationally will be required before ESI can be practically applied for high-quality, large-scale coatings.

ACKNOWLEDGEMENTS

The author gratefully acknowledges the support of a Naval Research Laboratory Postdoctoral Fellowship administered by the American Society for Engineering Education. Thanks are also given to J.P. Thomas for mentorship and to N. Charipar for helpful discussions.

REFERENCES

[1] Andreeva, D.V., Shchukin, D.G., 2008, "Smart Self-Repairing Protective Coatings", Materials Today, **11**, pp. 24-30.

[2] DeLongchamp, D.M., Hammond, P.T., 2004, "Multiple-Color Electrochromism from Layer-by-Layer-Assembled Polyaniline/Prussian Blue Nanocomposite Thin Films", Chemistry of Materials, 16, pp. 4799-4805.

[3] Choi, K., Yoo, S J., Sung, Y.-E., Zentel, R., 2006 "High Contrast Ratio and Rapid Switching Organic Polymeric Electrochromic Thin Films Based on Triarylamine Derivatives from Layer-by-Layer Assembly", Chemistry of Materials, **18**, pp. 5823-5825.

[4] Katsuhiko, A., Hill, J.P., Qingmin, J., 2007, "Layer-by-Layer Assembly as a Versatile Bottom-Up Nanofabrication Technique for Exploratory Research and Realistic Application", Physical Chemistry Chemical Physics, **9**, pp. 2319-2340.

[5] Jiang, C.Y., Tsukruk, V.V., 2006, "Freestanding Nanostructures via Layer-by-Layer Assembly", Advanced Materials, **18**, pp. 829-840.

[6] Lutkenhaus, J.L., Hammond, P.T., 2007, "Electrochemically Enabled Polyelectrolyte Multilayer Devices: From Fuel Cells to Sensors", Soft Matter, **3**, pp. 804-816.

[7] Merrill, M.H. and Sun, C.T., 2009, "Fast, Simple and Efficient Assembly of Nanolayered Materials and Devices" Nanotechnology, **20**, pp. 75606-75613.

[8] Rauschenbach, S., Stadler, F.L., Lunedei, E., Malinowski, N., Koltsov, S., Costantini, G., Kern, K., 2006, "Electrospray Ion Beam Deposition of Clusters and Biomolecules", Small, **2**, pp. 540-547.

[9] Jiang, W., Malshe, A.P., Brown, W.D., 2004, "Physical Powder Deposition of Solid Lubricant Nanoparticles by Electrostatic Spray Coating (ESC)", Surface and Coatings Technology, **177-178**, pp. 671-675.

[10] Fenn, J.B., 2002, "Electrospray Wings for Molecular Elephants", Les Prix Nobel, pp. 154-184.

[11] Swarbrick, J.C., Taylor, J.B., O'Shea, J. N., 2006, "Electrospray Deposition in Vacuum", Applied Surface Science, **252**, pp. 5622-5626.

[12] Lee, H.M., Kim, S.G., Matsui, I., Iwaki, T., Iskandar, F., Lenggoro, I.W., Okuyama, K., 2007, "Monolayer Deposition of L10 FePt Nanoparticles via Electrospray Route", Journal of Magnetism and Magnetic Materials, **313**, pp. 62-68.

[13] Mazumder, M.K., Sims, R.A., Biris, A.S., Srirama, P.K., Saini, D., Yurteri, C.U., Trigwell, S., De, S., Sharma, R., 2006, "Twenty-First Century Research Needs in Electrostatic Processes Applied to Industry and Medicine", Chemical Engineering Science, **61**, pp. 2192-2211.

[14] Lenggoro, I.W., Lee, H.M., Okuyama, K., 2006, "Nanoparticle Assembly On Patterned 'Plus/Minus' Surfaces from Electrospray of Colloidal Dispersion", Journal of Colloid and Interface Science, **303**, pp. 124-130.

[15] Suh, J., Han, B., Okuyama, K., Choi, M., 2005, "Highly Charging of Nanoparticles through Electrospray of Nanoparticle Suspension", Journal of Colloid and Interface Science, **287**, pp. 135-140.

[16] Nemes, P., Marginean, I., Vertes, A., 2007, "Spraying Mode Effect on Droplet Formation and Ion Chemistry in Electrosprays", Analytical Chemistry, **79**, pp. 3105-3116.

[17] Deng, W., Waits, C.M., Morgan, B., Gomez, A., 2009, "Compact Multiplexing of Monodisperse Electrosprays", Journal of Aerosal Science, **40**, pp. 907-918.

[18] Li, Y., Cole, R.B., 2003, "Shifts in Peptide and Protein Charge State Distributions with Varying Spray Tip Orifice Diameter in Nanoelectrospray Fourier Transform Ion Cycltron Resonance Mass Spectrometry", Analytical Chemistry, **75**, pp. 5739-5746.

[19] Peschke, M., Verkerk, U.H., Kebarle, P., 2004, "Features of the ESI Mechanism that Affect the Observation of Multiply Charged Noncovalent Protein Complexes and the Determination of the Association Constant by the Titration Method", Journal of the American Society for Mass Spectrometry, **15**, pp. 1424-1434.

[20] Ganan-Calvo, A.M., Lopez-Herrera Sanchez, J.M., 2003, "Device for the Production of Capillary Jets and Micro-and Nanometric Particles", US Patent No. 10503509.

[21] Ganan-Calvo, a.M., Lopez-Herrera, J.M., Riesco-Chueca, P., 2006, "The Combination of Electrospray and Flow Focusing", Journal of Fluid Mechanics, **566**, pp. 421-445.

[22] Lasheras, J.C., Hopfinger, E.J., 2000, "Liquid Jet Instability and Atomization in a Coaxial Gas Stream", Annual Review of Fluid Mechanics, **32**, pp. 275-308.

[23] Sazhin, S.S., 2006, "Advanced Models of Fuel Droplet Heating and Evaporation", Progress in Energy and Combustion Science, **32**, pp. 162-214.

[24] Ganan-Calvo, A.M., 2004, "On the General Scaling Theory for Electrospraying", Journal of Fluid Mechanics, **507**, pp. 203-212.

[25] Fernandez de la Mora, J., 2007, "The Fluid Dynamics of Taylor Cones", Annual Review of Fluid Mechanics, **39**, pp. 217-243.

[26] Collins, R.T., Jones, J.J., Harris, M.T., Basaran, O.A., 2008, "Electrohydrodynamic Tip Streaming and Emission of Charged Drops from Liquid Cones", Nature Physics, **4**, pp. 149-154.

[27] Hogan Jr., C.J., and Biswas, P., 2008, "Monte Carlo Simulation of Macromolecular Ionization by Nanoelectrospray", Journal of the American Society for Mass Spectrometry, **19**, pp. 1098-1107.

[28] Znamenskiy, V., Marginean, I., Vertes, A., 2003, "Solvated Ion Evaporation from Charged Water Nanodroplets", Journal of Physical Chemistry A, **107**, pp. 7406-7412.

[29] Tang, K., Smith, R.D., 1999, "Theoretical Prediction of Charged Droplet Evaporation and Fission in Electrospray Ionization", International Journal of Mass Spectrometry, **185-187**, pp. 97-105.

[30] Konermann, L., 2009, "A Simple Model for the Disintegration of Highly Charged Solvent Droplets During Electrospray Ionization", Journal of the American Society for Mass Spectrometry, **20**, pp. 496-506.

[31] Cech, N.B., Enke, C.G., 2001, "Effect of Affinity for Droplet Surfaces on the Fraction of Analyte Molecules Charged During Electrospray Droplet Fission", Analytical Chemistry, **73**, pp. 4632-4639.

[32] Deng, W., Gomez, A., 2007, "Influence of Space Charge on the Scale-Up of Multiplexed Electrosprays", Journal of Aerosol Science, **38**, pp. 1062-1078.

[33] Greendyke, R.B., Kaplan, C.R., 2006, "Simulation of Particulate Motion in Background Gas with Electrophoretic Forces by Hybrid CFD/MD Methods", Proc. of 44th AIAA Aerospace Sciences Meeting and Exhibit, AIAA 2006-1190.

[34] Wilhelm, O., Madler, L., Pratsinis, S.E., 2003, "Electrospray Evaporation and Deposition", Journal of Aerosol Science, **34**, pp. 815-836.

[35] Oh, H., Kim, K., Kim, S., 2008, "Characterization of Deposition Patterns Produced by Twin-Nozzle Electrospray", Journal of Aerosol Science, **39**, pp. 801-813.

[36] Rietveld, I.B., Kobayashi, K., Yamada H., Matsushige, K., 2006, "Electrospray Deposition, Model, and Experiment: Toward General Control of Film Morphology", Journal of Physical Chemistry B, **110**, pp. 23351-23364.

[37] Wilhelm, O., Pratsinis, S.E., Perednis, D., Gauckler, L.J., 2005, "Electrospray and Pressurized Spray Deposition of Yttria-Stabilized Zirconia Films", Thin Solid Films, **479**, pp. 121-129.

[38] Marginean, I., 2006, "From Chaotic Cone Pulsation to Ion Evaporation in Electrosprays", PhD Thesis, George Washington University.

[39] Kebarle, P., Verkerk, U.H., 2009, "Electrospray: From Ions in Solution to Ions in the Gas Phase, What We Know Now", Mass Spectrometry Reviews, **28**, pp. 898-917.

[40] Hogan, Jr., C.J., Carroll, J.A., Rohrs, H.W., and Biswas, P., Gross, M.L., 2009, "Combined Charged Residue-Field Emission Model of Macromolecular Electrospray Ionization", Analytical Chemistry, **81**, pp. 369-377.

[41] Law, S.E., 2001, "Agricultural Electrostatic Spray Application: A Review of Significant Research and Development During the 20th Century", Journal of Electrostatics, **51-52**, pp. 25-42.

[42] Quere, D., 2008, "Wetting and Roughness", Annual Review of Materials Research, **38**, pp. 71-99.

[43] Harper, J.D., 2009, "Characterization and Design of Low-Temperature Plasma Based Probes for Ambient Sampling of Chemicals", Masters Thesis, Purdue University.

